SCIENTIFIC REPORTS

OPEN

SUBJECT AREAS:
TECTONICS
GEOCHEMISTRY
GEODYNAMICS
GEOLOGY

Received
9 January 2013

Accepted
4 February 2013

Published
19 February 2013

Correspondence and requests for materials should be addressed to H.I. (ito_hisa@criepi.denken.or.jp)

Earth's youngest exposed granite and its tectonic implications: the 10–0.8 Ma Kurobegawa Granite

Hisatoshi Ito[1], Ryuji Yamada[2], Akihiro Tamura[3], Shoji Arai[3], Kenji Horie[4] & Tomokazu Hokada[4]

[1]Geosphere Science Sector, Central Research Institute of Electric Power Industry, Chiba 270-1194, Japan, [2]National Research Institute for Earth Science and Disaster Prevention, Ibaraki 305-0006, Japan, [3]Department of Earth Sciences, Kanazawa Univ., Ishikawa 920-1192, Japan, [4]National Institute of Polar Research, Tokyo 190-8518, Japan.

Although the quest for Earth's oldest rock is of great importance, identifying the youngest exposed pluton on Earth is also of interest. A pluton is a body of intrusive igneous rock that crystallized from slowly cooling magma at depths of several kilometers beneath the surface of the Earth. Therefore, the youngest exposed pluton represents the most recent tectonic uplift and highest exhumation. The youngest exposed pluton reported to date is the Takidani Granodiorite (~ 1.4 Ma) in the Hida Mountain Range of central Japan. Using LA-ICP-MS and SHRIMP U-Pb zircon dating methods, this study demonstrates that the Kurobegawa Granite, also situated in the Hida Mountain Range, is as young as ~ 0.8 Ma. In addition, data indicate multiple intrusion episodes in this pluton since 10 Ma with a ~ 2-million-year period of quiescence; hence, a future intrusion event is likely within 1 million years.

The Hida Mountain Range (HMR; Fig. 1) is the largest and highest mountain system in Japan and is located to the west of the plate-bounding Itoigawa-Shizuoka Tectonic Line (ISTL). High mountains of up to ~ 3000 m face the Japan Sea with a deep basin of ~ 1000 m depth (the Toyama Trough) located within 50 km. The HMR is known to have the highest uplift and denudation rates during the Quaternary in Japan[1,2]. Granite is the dominant lithology in the HMR and many stages of granitic magma intrusion have been recognized, namely, ~ 190 Ma, ~ 100 Ma, ~ 90 Ma, ~ 70 Ma, 65–60 Ma, ~ 5 Ma, ~ 3 Ma, and 2–1 Ma[3]. These ages were largely determined by K-Ar and fission-track dating methods[4–7] with relatively low closure temperatures and hence predominantly postdate the magmatic intrusions. Only a few zircon U-Pb ages have been obtained in the HMR[8,9]. Therefore, the exact timing of magmatic intrusion in the HMR has been unclear.

Two stages of mountain building have been assumed for the Quaternary tectonics in the HMR: a period of magmatic intrusion from 2.7–1.5 Ma, followed by a period of E–W compressional stress from 1.4–0.5 Ma[10–12]. The Takasegawa fault (Fig. 1), a tectonic lineament, lies parallel to the ISTL in the middle of the HMR, and granitic rocks are mylonitized along the lineament[9,10]. It is thought that E–W stress since 1.4 Ma caused the eastern part of the HMR to be tilted eastward and pushed up along this lineament, exposing deeper sections of the granite[3,11].

The Kurobegawa Granite is a batholithic pluton exposed over an area of ~ 100 km^2 in the HMR (Fig. 1). Although the Kurobegawa Granite proper is commonly restricted to the Quaternary intrusion[3] to the west of the Jiigatake Volcanic Rocks, it is broadly referred to as the Neogene granite[6]. The pluton extends to the main ridgeline of the HMR in the east and is deeply eroded in the west, with vertical exposures ranging from 700 to 2900 m in elevation. The Kurobegawa Granite is divided into 3 units (upper, middle, and lower), steeply tilted eastward, exposing deeper section toward the west[12,13]. The emplacement depth of the pluton is inferred to be 4–10 km[12,13].

Recently obtained reliable K-Ar ages[3] for the Kurobegawa Granite show a hornblende age of 0.57 ± 0.38 Ma (error: 2σ) and biotite ages of 0.58 ± 0.04 Ma, 0.62 ± 0.06 Ma, 0.65 ± 0.06 Ma, and 0.66 ± 0.06 Ma at the southwestern rim of the granite (near the sampling site KRG22: Fig. 1). The Kurobegawa Granite intrudes 1.55 ± 0.28 Ma volcanic rocks (the Jiigatake Volcanic Rocks; dated by K-Ar groundmass) at its eastern border[3]. From these data, the emplacement time of the Kurobegawa Granite was roughly assumed to be 1.7–0.9 Ma[3].

In the present study, a total of 34 granitic rocks and one volcanic rock (from the Jiigatake Volcanic Rocks) were dated by the U-Pb method on zircons using LA-ICP-MS (laser ablation inductively coupled plasma mass spectrometry) with a 40 μm laser beam. All of the samples were collected in and around the Kurobegawa Granite (Fig. 1).

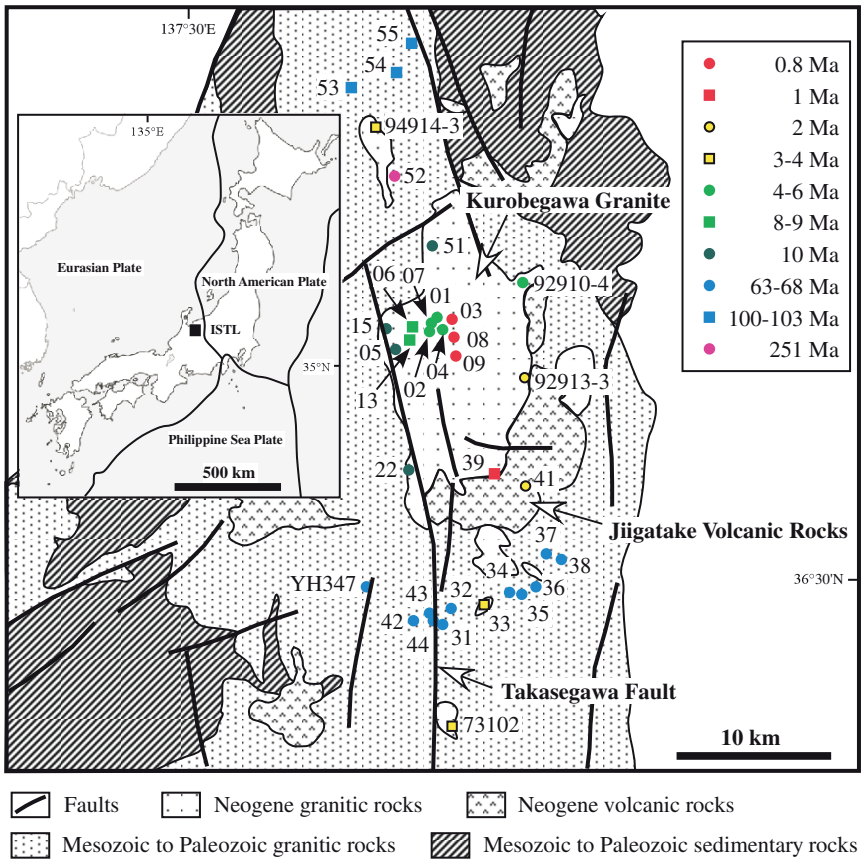

Figure 1 | Location of the study site (inset) and geological map[42] of the Hida Mountain Range showing the sample locations and U-Pb ages. Sample names are shown near the sampling point; two-digit numbers indicate KRG samples. U-Pb ages older than 1 Ma are rounded to the nearest Ma.

Results

Figure 1 shows the distribution of the U-Pb ages obtained in this study. The youngest U-Pb ages are located in the central part of the Kurobegawa Granite, from sampling sites KRG03, KRG08, and KRG09. The U-Pb ages of samples from KRG03, KRG08, and KRG09 are 0.81 ± 0.09 Ma, 0.81 ± 0.09 Ma, and 0.77 ± 0.03 Ma, respectively (Supplementary Table S2). The age of sample KRG08 was cross-checked using a 20 μm laser beam, yielding a similar age of 0.70 ± 0.08 Ma (Fig. 2; Supplementary Table S3). The accuracy of the dating result for sample KRG08 was also supported by SHRIMP U-Pb data (Fig. 2; Supplementary Table S4). From these data it seems reasonable to assume that the zircons crystallized from the magma at ~ 0.8 Ma. This demonstrates that the latest intrusion of the Kurobegawa Granite (~ 0.8 Ma) is younger than the Takidani Granodiorite (~ 1.4 Ma[8]; located ~ 25 km to the south of the Kurobegawa Granite), making it the youngest exposed granite on Earth to the best of our knowledge.

A total of 340 zircon grains from granitic rocks were dated using a 40 μm laser beam (Supplementary Table S2). Four analyses were excluded because of exceptionally large error values, three grains gave ages older than 1430 Ma, and 13 grains gave ages between 148 and 273 Ma. Figure 3 shows the U-Pb grain age distributions for the 320 zircons younger than 140 Ma. For zircons that gave ages older than 20 Ma, there were two peaks at 65 Ma and 100 Ma. As shown in Figure 1, granites of ~ 65 Ma are widely distributed to the south of the Kurobegawa Granite, whereas ~ 100 Ma granites are present to the north of the Kurobegawa Granite. Stock-sized plutons of ~ 3 Ma were locally emplaced both to the north and south of the Kurobegawa Granite (94914-3, KRG33, 73102).

Discussion

Figure 3b shows U-Pb grain age distributions for zircons that are younger than 20 Ma. There are peaks at 0.8, 1.3, 3.3, 5.5, 7.9, and 9.5 Ma. It is clear that there were multiple episodes of magmatic intrusion over the last 10 million years. It is interesting that in Japan ~ 15 Ma granites related to the opening of the Japan Sea are widely distributed[14], whereas these are absent in the HMR and instead Neogene granitic intrusion occurred since ~ 10 Ma. From the periodic intrusion episodes since 10 Ma in the HMR, it is plausible that a future intrusion event is likely within 1 million years.

A transect that runs through the middle of the Kurobegawa Granite from the central part to the western rim shows a considerable age difference (Fig. 1). All three samples in the central part (KRG03, 08, 09) gave dates of ~ 0.8 Ma. It should be noted that among these, KGB03 had a grain that gave an age of ~ 65 Ma and KGB09 had a grain that gave an age of ~ 2 Ma. Because these ages are consistent with older granite emplacement periods, we assume they are xenocrysts[15] that represent older magmatic activity. Within a few kilometers west of the ~ 0.8 Ma granite, four samples (KRG01, 02, 04, and 07) gave ages of 4–6 Ma. It should be noted that among these, KRG01 had a grain that gave an age of ~ 65 Ma and KRG04 had a grain that gave an age of ~ 10 Ma. These are also xenocrysts that represent older magmatic activity. A few kilometers west of the 4–6 Ma granite, two samples (KRG06, and 13) gave ages of 8–9 Ma. Immediately to the west of the 8–9 Ma granite, a sample (KRG05) gave an age of ~ 10 Ma, and an aplitic sample (KRG15) gave grain ages of ~ 10 Ma, ~ 65 Ma, and > 175 Ma. The abundant xenocrysts in sample KRG15 is a reflection of the sample site's location on the western rim of the Kurobegawa Granite, making it susceptible to intermingling with country rocks during magmatic ascent. An age of ~ 10 Ma was obtained at a northern (KRG51) and a southern (KRG22) site at the western rim of the Kurobegawa Granite, demonstrating that ~ 10 Ma magma was common at the western rim of the Kurobegawa Granite. The eastward-younging phenomenon may support the model of the Kurobegawa Granite being tilted eastward

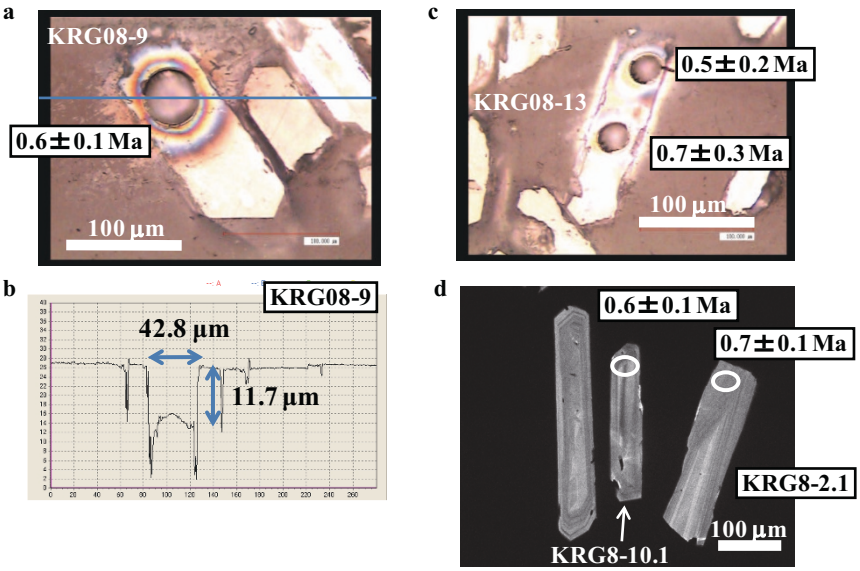

Figure 2 | Images of zircons that gave ages of ~ 0.8 Ma. U-Pb ages (2σ error) were obtained using a 40 μm laser beam (a) that created pits of ~ 12 μm in depth (b). Some samples were also dated using a 20 μm laser beam both at the center and at the rim (c). SHRIMP using a 40 μm ion beam (white circle) (d) also yielded ages consistent with those by LA-ICP-MS (a, c). Ages shown are not corrected for initial ^{230}Th disequilibrium. After this correction, the ages become ~ 0.1 Ma older (Supplementary Tables S2, S3). Cathodoluminescence images (d) showed weak oscillatory zoning without any inherited cores.

during the Quaternary exposing deeper sections of the granite toward the west[3,12], assuming that upward-younging incremental emplacements occurred horizontally[16,17]. This argument may be further corroborated by a prevalence of mylonitic structures at the western rim of the Kurobegawa Granite. In addition, K-Ar hornblende and biotite dating methods gave a similar age of ~ 0.6 Ma[3] at the southwestern rim of the granite, indicating rapid uplift and erosion during this time.

We obtained ages of 5.4 Ma (sample name: 92910-4), 2.2 Ma (92913-3), and 1.3 Ma (KRG39) at the eastern rim of the Kurobegawa Granite. This shows that several discrete intrusions occurred there, making it difficult to assume that horizontal sheet-like intrusions occurred at these locations. Some of these samples contained ~ 65 Ma xenocrysts. Because xenocrysts of ~ 65 Ma are ubiquitous in the Kurobegawa Granite, granitic magmatism at ~ 65 Ma was widespread and therefore a ~ 65 Ma granite body must exist beneath the Kurobegawa Granite. Granite emplacements of ~ 100 Ma and ~ 250 Ma were confirmed to the north of the Kurobegawa Granite.

In conclusion, the U-Pb age data demonstrate that the Kurobegawa Granite was not formed by the crystallization of large-volume magma chambers but rather was emplaced incrementally through the amalgamation of many intrusions over millions of years[18–20]. The latest intrusion event was ~ 0.8 Ma. The rapid uplift and erosion of the HMR in the Quaternary was caused by not only compressional stress but also magmatic intrusion.

Methods

LA-ICP-MS U-Pb dating. Zircons were extracted by conventional heavy liquid and magnetic separations. They were handpicked and embedded in a PFA Teflon sheet and slightly polished (by ~ 1 μm) by diamond paste 6 μm in diameter.

LA-ICP-MS U-Pb dating was performed at Kanazawa University, Japan, using an Agilent 7500s quadrupole ICP-MS coupled to a MicroLas GeoLas Q plus excimer ArF laser system[21] (Supplementary Table S1). Samples were ablated by pulses at a 5 Hz repetition rate with an energy density of 8 J/cm^2 in helium gas. Data were acquired in peak jumping mode over 270 mass scans during a 30 s background measurement, followed by 30 s sample ablation and then a 40 s background measurement using a 40 μm spot-size and instrumental parameters as shown in Supplementary Table S1. To augment the accuracy of data analyses, duplicate dating using a 20 μm spot-size were performed for seven samples.

Data for the first 5 s of ablation were neglected to avoid surface contamination and signal instability, and the following 10 s of data were used for age calculation. Approximately 12 μm was drilled for the 30 s laser ablation (Fig. 2) and therefore data from 2–6 μm depths were analyzed.

Raw data were processed offline using an Excel spreadsheet program created by the first author. After gas blank correction, laser-induced elemental fractionation and instrumental mass discrimination were corrected by normalization to the Fish Canyon Tuff (FCT) zircon[22]. The drift of the Pb/U ratio during the analytical session was monitored and corrected by the NIST SRM 610 glass standard, which was analyzed every 10 laser ablations.

We used FCT zircon as a U-Pb reference material because it has been precisely dated by the ID-TIMS U-Pb method[22] and our repeated analyses of FCT confirmed its suitability as a U-Pb reference zircon[9,23]. To test the validity of the applied method and the reproducibility of the obtained age data, zircons of known age from the Buluk Member Tuff (16.2 ± 0.6 Ma[24]) were also dated during the analytical session. The agreement of the results (Supplementary Tables S2, S3) with the reference age supports the validity of our dating methodology.

Data processing and age calculations were completed using Isoplot v. 3.75[25]. Individual ^{238}U-^{206}Pb grain ages were determined using the ^{206}Pb/^{238}U ratio, and the error was calculated based on the time-series fluctuation (standard error) of ^{206}Pb/^{238}U for the time range adopted (i.e., 35–45 s). Common-lead correction was done using the ^{207}Pb method[26,27]. A common-lead corrected age was also obtained for each sample using the Tera-Wasserburg plot[28,29] (Supplementary Figure S1), in which the upper intercept age was anchored to give an initial common ^{207}Pb/^{206}Pb ratio of 0.83[30]. For the 20 μm laser ablation, data were obtained from both the center and rim of a grain so that two ages were obtained for a single grain (Fig. 2). Ten ages for five grains were obtained for each sample (Supplementary Table S3).

It should be mentioned that young (e.g., < 2 Ma) U-Pb zircon ages are strongly affected by disequilibrium of ^{230}Th at the time of zircon crystallization from the magma[31]. Therefore, individual zircon U-Pb ages of samples that were less than 2 Ma were corrected using a factor f, where $f = (\mathrm{Th/U})_{\mathrm{zircon}}/(\mathrm{Th/U})_{\mathrm{magma}}$[31]. The $(\mathrm{Th/U})_{\mathrm{magma}}$ was assumed to be 4.8, which was an average derived from river sand samples collected in the vicinity of the Kurobegawa Granite[32]. The $(\mathrm{Th/U})_{\mathrm{zircon}}$ was substituted by the measured ^{232}Th/^{238}U of individual zircons. The corrected age is mostly ~ 0.1 Ma older than the corresponding uncorrected age (Supplementary Tables S2, S3).

Ages from the center and rim of a grain show similarity for most samples, especially in grains younger than 10 Ma (Supplementary Table S3). Therefore, we assume ages < 10 Ma are unaffected by inheritance[33]. The low values (mostly < 6) of mean squared weighted deviates (MSWD[34]; Supplementary Tables S2, S3) for sample ages < 10 Ma also indicate that the influence of inheritance is small. Some grains older than ~ 60 Ma show a large age discrepancy within the grain (e.g., KRG31-11c and KRG31-11r in Supplementary Table S3), which indicates inheritance. Moreover, MSWDs for samples > 65 Ma show high values (mostly > 10) which are probably due to inherited and xenocrystic zircons[15,33]. Because our interest in this study is magmatism during the Neogene, we do not address ages older than 65 Ma in detail.

SHRIMP U-Pb dating. Two samples (KRG04 and KRG08) were also dated using a sensitive high resolution ion microprobe (SHRIMP II) at the National Institute of

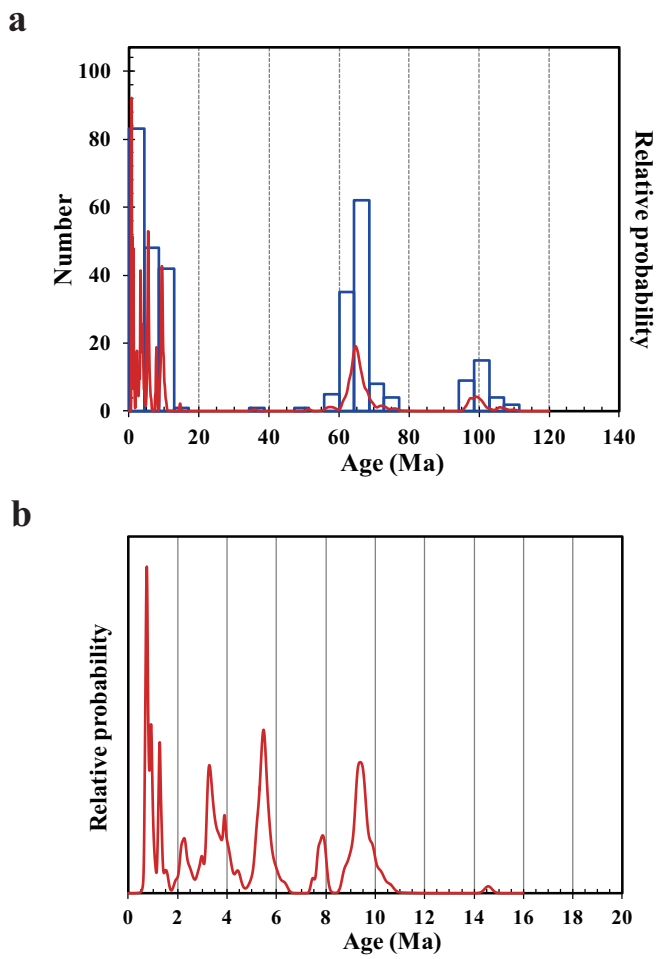

Figure 3 | Age distribution of individual zircons. (a), Age distributions (cumulative probability distributions[25]) for 320 grains of granitic origin with ages younger than 140 Ma. The peaks > 20 Ma are at 65 and 100 Ma. (b), Age distributions for 174 grains with ages younger than 20 Ma. The prominent peaks are 0.8, 1.3, 3.3, 5.5, 7.9, and 9.5 Ma.

Polar Research (NIPR), Japan. Procedures of sample preparation and zircon analysis essentially follow those described previously[35]. Zircon grains were mounted and polished together with standards in an epoxy resin disc. To investigate the internal structures of individual zircons, backscattered electron and cathodoluminescence images were obtained using a scanning electron microscope (JEOL JSM-5900LV) at NIPR. These images guided the selection of points for analysis. The surfaces of grain mounts were washed with 2% HCl to remove any lead contamination and then coated with gold prior to analysis. An O_2^- primary ion beam of 8 nA was used to sputter an analytical spot of 40 μm diameter on the polished mount. The procedures for Pb and U isotopic analyses of zircon follow previous studies[26,36,37]. In the present study, TEMORA2 ($^{206}Pb/^{238}U$ age = 416.8 Ma[38]) and SL13 (U concentration 238 ppm[39]) were used as calibration standard materials for the U-Pb analysis. The U-Pb data were reduced in a manner similar to that described previously[26], using SQUID 2[40]. A correction for common Pb was made by assuming $^{206}Pb/^{238}U$-$^{207}Pb/^{235}U$ age-concordance and the model for common Pb compositions proposed by the bulk-crust Pb isotope composition model[41]. The pooled ages presented in the present study are all after correction for common Pb and were calculated using the Isoplot 3.75 software[25]. A common Pb-corrected weighted mean age of 5.4 ± 0.1 Ma (MSWD = 1.3) was obtained for sample KRG04 (Supplementary Table S4). This is in good agreement with the LA-ICP-MS age of 5.5 ± 0.1 Ma (Supplementary Table S2). A common Pb-corrected weighted mean age of 0.68 ± 0.02 Ma (MSWD = 1.1) was obtained for sample KRG08 (Supplementary Table S4). This is also in good agreement with the LA-ICP-MS age of 0.70 ± 0.08 Ma (before initial ^{230}Th disequilibrium correction) using a 40 μm laser beam (Supplementary Table S2). The remarkable agreement between SHRIMP and LA-ICP-MS ages support the reliability of the LA-ICP-MS U-Pb ages in this study.

1. Ohmori, H. Mean Quaternary uplift rates in the central Japanese mountains estimated by means of geomorphological analysis. *Bull. Dept. Geogr., Univ. Tokyo* **no.19**, 29–36 (1987).
2. Ohmori, H. The paradox of equivalence of the Davisian end-peneplain and Penckian primary peneplain. In: Evans, I. S., Dikau, R., Tokunaga, E., Ohmori, H. & Hirano, M. (eds.): *Concepts and Modelling in Geomorphology: International Perspectives*, TERRAPUB, Tokyo, pp. 3–32 (2003).
3. Harayama, S., Takahashi, M., Shukuwa, R., Itaya, T. & Yagi, K. High-temperature hot springs and Quaternary Kurobegawa Granite along the Kurobegawa River. *J. Geol. Soc. Japan* **116**, Supplement 63–81 (2010).
4. Ogata, S., Miyakoshi, K., Shidahara, T. & Tanaka, K. Geology of the Kurobe geothermal area. *Central Res. Inst. Electric Power Industry Rep.* **382032**, 27p (1983).
5. Nishimura, S. & Mogi, T. The interpretation of discordant ages of some granitic bodies. *J. Geotherm. Res. Soc. Japan* **8**, 145–164 (1986).
6. Uchiumi, S., Harayama, S. & Uto, K. K-Ar dating on age-unknown rocks in the 1 : 200,000 quadrangle, Toyama. *Bull. Geol. Surv. Japan* **46**, 375–381 (1995).
7. Yamada, R. & Harayama, S. Fission track and K-Ar dating on some granitic rocks of the Hida Mountain Range, central Japan. *Geochem. J.* **33**, 59–66 (1999).
8. Sano, Y., Tsutsumi, Y., Terada, K. & Kaneoka, I. Ion microprobe U-Pb dating of Quaternary zircon: implication for magma cooling and residence time. *J. Volcanol. Geotherm. Res.* **117**, 285–296 (2002).
9. Ito, H., Tamura, A., Morishita, T. & Arai, S. Timing of some plutonic intrusions and tectonics in the Hida Mountain Range: An application of LA-ICP-MS U-Pb dating on zircons. *J. Geol. Soc. Japan* **118**, 449–456 (2012).
10. Yamada, R. 1999. Cooling history analysis of granitic rock in the Northern Alps, central Japan. *The earth monthly* **21**, 803–810 (1999).
11. Harayama, S., Ohyabu, K., Miyama, Y., Adachi, H. & Shukuwa, R. Eastward tilting and uplifting after the late Early Pleistocene in the eastern-half area of the Hida Mountain Range. *Quarter. Res.* **42**, 127–140 (2003).
12. Harayama, S., Wada, H. & Yamaguchi, Y. Quaternary and Pliocene granites in the Northern Japan Alps. Hutton Symposium V, Field Guidebook, Trip A1. *Geol. Surv. Japan, Interim-Rep.* **28**, 3–21 (2003).
13. Wada, H., Harayama, S. & Yamaguchi, Y. Mafic enclaves densely concentrated in the upper part of a vertically zoned felsic magma chamber: The Kurobegawa granitic pluton, Hida Mountain Range, central Japan. *Bull. Geol. Soc. Amer.* **116**, 788–801 (2004).
14. Kimura, J.-I., Stern, R. J. & Yoshida, T. Reinitiation of subduction and magmatic responses in SW Japan during Neogene time. *Bull. Geol. Soc. Amer.* **117**, 969–986 (2005).
15. Miller, J. S., Matzel, J. E. P., Miller, C. F., Burgess, S. D. & Miller, R. B. Zircon growth and recycling during the assembly of large, composite arc plutons. *J. Volcanol.Geotherm. Res.* **167**, 282–299 (2007).
16. Wiebe, R. A. & Collins, W. J. Depositional features and stratigraphic sections in granitic plutons: implications for the emplacement and crystallization of granitic magma. *J. Struct. Geol.* **20**, 1273–1289 (1998).
17. Petford, N., Cruden, A. R., McCaffrey, K. J. W. & Vigneresse, J.-L. Granite magma formation, transport and emplacement in the Earth's crust. *Nature* **408**, 669–673 (2000).
18. Coleman, D. S., Gray, W. & Glazner, A. F. Rethinking the emplacement and evolution of zoned plutons: Geochronologic evidence for incremental assembly of the Tuolumne Intrusive Suite, California. *Geology* **32**, 433–436 (2004).
19. Glazner, A. F., Bartley, J. M., Coleman, D. S., Gray, W. & Taylor, R. Z. Are plutons assembled over millions of years by amalgamation from small magma chambers? *GSA Today* **14**, 4–11(2004).
20. Davis, J. W., Coleman, D. S., Gracely, J. T., Gaschnig, R. & Stearns, M. Magma accumulation rates and thermal histories of plutons of the Sierra Nevada batholith, CA. *Contrib. Mineral. Petrol.* **163**, 449–465 (2012).
21. Morishita, T., Ishida, Y., Arai, S. & Shirasaka, M. Determination of multiple trace element compositions in thin (< 30 μm) layers of NIST SRM 614 and 616 using laser ablation-inductively coupled plasma-mass spectrometry (LA-ICP-MS). *Geostandards Geoanalytical Res.* **29**, 107–122 (2005).
22. Schmitz, M. D. & Bowring, S. A. U-Pb zircon and titanite systematics of the Fish Canyon Tuff: an assessment of high-precision U-Pb geochronology and its application to young volcanic rocks. *Geochim. Cosmochim. Acta* **65**, 2571–2587 (2001).
23. Ito, H., Tamura, A., Morishita, T. & Arai, S., Zircon U-Pb and fission-track ages of granitic rocks from the Nojima Fault and its vicinity: A new horizon for the LA-ICP-MS U-Pb dating method. *J. Geol. Soc. Japan* **116**, 544–551 (2010).
24. Hurford, A. J. & Watkins, R. T. Fission-track age of the tuffs of the Buluk Member, Bakate Formation, Northern Kenya: a suitable fission-track age standard. *Chem. Geol.(Isot. Geosci. Sect.)* **66**, 209–216 (1987).
25. Ludwig, K. R. User's Manual for Isoplot 3.75: A geochronological toolkit for Microsoft Excel. *Berkeley Geochronology Center Spec. Pub.* **5**, 75p (2012).
26. Williams, I. S., U–Th–Pb geochronology by ion microprobe. In: McKibben, M. A., Shanks III, W. C. & Ridley, W. I. (eds.): Applications of Microanalytical Techniques to Understanding Mineralizing Processes. *Reviews in Economic Geology* **7**, pp. 1–35 (1998).
27. Cocherie, A., Fanning, C. M., Jezequel, P. & Robert, M. LA-MC-ICPMS and SHRIMP U–Pb dating of complex zircons from Quaternary tephras from the French Massif Central: Magma residence time and geochemical implications. *Geochim. Cosmochim. Acta* **73**, 1095–1108 (2009).
28. Tera, F. & Wasserburg, G. J. U-Th-Pb systematics in three Apollo 14 basalts and the problem of initial Pb in lunar rocks. *Earth Planet. Sci. Lett.* **14**, 281–304 (1972).

29. Jackson, S. E., Pearson, N. J., Griffin, W. L. & Belousova, E. A. The application of laser ablation-inductively coupled plasma-mass spectrometry to in situ U-Pb zircon geochronology. *Chem. Geol.* **211**, 47–69 (2004).
30. Cumming, G. L. & Richards, J. R. Ore lead isotope ratios in a continuously changing Earth. *Earth Planet. Sci. Lett.* **28**, 155–171 (1975).
31. Scharer, U. The effect of initial ^{230}Th disequilibrium on young U-Pb ages: The Makalu case, Himalaya. *Earth Planet. Sci. Lett.* **67**, 191–204 (1984).
32. Imai, N. *et al*. Geochemical map of Japan. *Geological Survey of Japan, AIST*, 209p (2004).
33. Gaschnig, R. M., Vervoort, J. D., Lewis, R. S. & McClelland, W. C. Migrating magmatism in the northern US Cordillera: in situ U–Pb geochronology of the Idaho batholith. *Contrib. Mineral. Petrol.* **159**, 863–883 (2010).
34. Wendt, I. & Carl, C. The statistical distribution of the mean squared weighted deviation. *Chem. Geol. (Isot. Geosci. Sect.)* **86**, 275–285 (1991).
35. Horie, K., Hokada, T., Hiroi, Y., Motoyoshi, Y. & Shiraishi, K. Contrasting Archaean crustal records in western part of the Napier Complex, East Antarctica: New constraints from SHRIMP geochronology. *Gondwana Res.* **21**, 829–837 (2012).
36. Compston, W., Williams, I. S. & Meyer, C. U–Pb geochronology of zircons from lunar breccia 73217 using a sensitive high mass-resolution ion microprobe. *J. Geophys.Res.* **89**, 525–534 (1984).
37. Horie, K., Hidaka, H. & Gauthier-Lafaye, F. Elemental distribution in zircon: Alteration and radiation-damage effects. *Physics Chem. Earth* **31**, 587–592 (2006).
38. Black, L. P. *et al*. Improved ^{206}Pb/^{238}U microprobe geochronology by the monitoring of a trace-element-related matrix effect; SHRIMP, ID-TIMS, ELA-ICP-MS and oxygen isotope documentation for a series of zircon standards. *Chem. Geol.* **205**, 115–140 (2004).
39. Claoue-Long, J. C., Compston, W., Roberts, J. & Fanning, C. M. Two Carboniferous ages: a comparison of SHRIMP zircon dating with conventional zircon ages and ^{40}Ar/^{39}Ar analysis. In: Berggren, W. A., Kent, D. V., Aubry, M.-P. & Hardenbol, J. (eds.): *Geochronology Time Scales and Global Stratigraphic Correlation*, Society for Sedimentary Geology Special Publication, No. **54**, pp. 3–21 (1995).
40. Ludwig, K. R. SQUID 2 (rev. 2.50): A User's Manual. *Berkeley Geochronology Center. Spec. Pub.* **5**, 104p (2009).
41. Stacey, J. S. & Kramers, J. D. Approximation of terrestrial lead isotope evolution by a two-stage model. *Earth Planet. Sci. Lett.* **26**, 207–221 (1975).
42. Geological Survey of Japan, AIST (ed.). Seamless digital geological map of Japan 1: 200,000. Jun 29, 2011 version. Research Information Database DB084, Geological Survey of Japan, National Institute of Advanced Industrial Science and Technology (2011).

Acknowledgments

We thank S. Harayama for providing us with some of the samples from Hida Mountain Range.

Author contributions

H.I. analyzed LA-ICP-MS U-Pb data and primarily wrote the manuscript. R.Y. collected zircons and performed the LA-ICP-MS experiment with A.T. S.A. supervised the LA-ICP-MS analyses. K.H. and T.H. performed SHRIMP analyses. All authors contributed to writing the manuscript.

Additional information

Supplementary information accompanies this paper at http://www.nature.com/scientificreports

Competing financial interests: The authors declare no competing financial interests.

How to cite this article: Ito, H. *et al*. Earth's youngest exposed granite and its tectonic implications: the 10–0.8 Ma Kurobegawa Granite. *Sci. Rep.* **3**, 1306; DOI:10.1038/srep01306 (2013).